OECC/ACOFT 2014 – Melbourne, 6-10 July

Welcome

The OptoElectronics and Communication Conference and Australian Conference on Optical Fibre Technology 2014 Organising Committee thank you for your valued contribution to the Conference.

Conference Hosted by

ENGINEERS AUSTRALIA

THE AUSTRALIAN OPTICAL SOCIETY

Technical Co-Sponsors

IEEE photonics SOCIETY

OSK 사단법인 한국광학회 Optical Society of Korea

IEICE Communications Society

OSA The Optical Society

EIC

Cooperating Organisation

SPIE

	CONCURRENT SESSION 7						
	WE7A	WE7B	WE7C	WE7D	WE7E	WE7F	WE7G
1030-1200	**Elastic Optical Networks II**	**Nonlinear Fibre Devices I**	**Quantum Dot and Advanced Laser Sources**	**Biophotonics**	**Silicon Waveguide Devices**	**Optical Signal Processing**	**G Tutorials**
	Meeting Room 101 / 102	*Meeting Room 105*	*Meeting Room 106*	*Meeting Room 103*	*Meeting Room 104*	*Meeting Room 107*	*Plenary 1*
1030-1045	WE7A1 *Single Span Transmission of Real-time 1.2 Tb/s Nyquist WDM Signal over 4 Types of Optical Fiber* **Yiran Ma**	WE7B1 *Silicon Fiber Devices for Nonlinear Applications* **Anna Peacock** Invited Speaker	WE7C1 *Complexity Analysis of a Photonic Integrated Chaotic Laser and Related Nonlinear Laser Systems* **Deb Kane**	WE7D1 *Deep Tissue Multiphoton Imaging* **Chris Xu** Invited Speaker	WE7E1 *Low-Loss All-Adiabatic Silicon-Waveguide Polarization-Division Multiplexer in C and L Bands* **Akira Oka** Invited Speaker	WE7F1 *Wavelength Conversion of RZ-DPSK Signal with Pulsewidth Tunability Using Four Wave Mixing and Raman Amplifier Based Pulse Compressor* **G.M. Sharif**	WE7G1 *Ultrahigh Spectral Efficiency Systems - Pushing the Limits of Multi-level Modulation, Multi-core Fiber, and Multi-mode Control* **Masataka Nakazawa**
1045-1100	WE7A2 *Supporting Dynamic Traffic Over Super-channels in Flexible Grid Optical Networks* **Philip N. Ji**		WE7C2 *Optical Bandwidth Enhancement at High-temperature Operation of Light Emitting-Transistors* **Te Lee**			WE7F2 *6-Fold Wavelength Multicasting Using Tunable-Width Picosecond Pulse Source from Raman Adiabatic-Soliton-Compressor* **Irneza Ismail**	
1100-1115	WE7A3 *Impact of Adding/Dropping Nyquist-WDM Superchannels on Transmission Performance in an Elastic Optical Network* **Masahiko Jinno**	WE7B2 *Amplification of DWDM Channels Using a Bidirectional Fiber Optical Parametric Amplifier* **Gordon Lei**	WE7C3 *Advances in Quantum Dot Lasers for Telecom and Silicon Photonics Application* **Yasuhiko Arakawa** Invited Speaker	WE7D2 *Fluorescent Nanoparticles for Biological Applications* **Ewa Goldys** Invited Speaker	WE7E2 *Low Transmission Loss Silicon Slot Waveguide Operating at 1064nm* **Xiangdong Li**	WE7F3 *Coherently-Pumped 20Gbaud 16QAM Optical Wavelength Shifting Free of Phase Noise from Pumps* **Guo-Wei Lu**	
1115-1130	WE7A4 *Distance-adaptive Spectrum Slot Allocation Algorithm for Efficient Use of Network Resources on Elastic Optical Network* **Shinsuke Fujisawa**	WE7B3 *Temporal Cavity Solitons Used as a 10 Gb/s All-optical Buffer* **Stuart Murdoch**			WE7E3 *Compact Deep Etched Silicon Circular Reflector with High Reflection and Wide Bandwidth* **Shitao Gao**	WE7F4 *OSNR and CD-Tolerant All-Optical 40 Gb/s Clock Recovery by using an Amplified-Feedback Laser* **Yuan Bo**	
1130-1145	WE7A5 *Transport SDN Enabled by Flexible Optical System* **Philip N. Ji** Invited Speaker	WE7B4 *Multichannel Tunable Pulsewidth NRZ-to-RZ Conversion of Intensity and Phase-Modulated Signals Using Raman Adiabatic-Soliton Compressor* **Irneza Ismail**	WE7C4 *1.5 Âµm High-gain Quantum Dot Materials and Devices for Future High-capacitance Optical Communications Systems* **Johann Peter Reithmaier** Invited Speaker	WE7D3 *Optically Driven Mechanical Micro and Nanosystems* **Halina Rubinsztein-Dunlop** Invited Speaker	WE7E4 *Evanescent Wave Sensors Utilizing Laterally Radiating Thin-ridge Silicon-on-Insulator Waveguide Tapers* **Kiplimo Yego**	WE7F5 *Hybrid Fiber Optical Parametric Amplifiers for Optical Communication* **Michel E. Marhic** Invited Speaker	
1145-1200		WE7B5 *Cascaded Operation of Wavelength Converter for Dual-Polarization Phase-Modulated Signal* **Hung Nguyen Tan**			WE7E5 *Compact Beam Splitters Based on a Simple Silicon Slit Structure* **Toshio Katsuyama**		
1200-1300	**Lunch** *(Lunch not provided)*						
1300-1400	WEPS2 **Poster Session II** *Level 1 Foyer*						

WEPS2: Poster Session II continued ...

WEPS2: Poster Session II continues next page ...

Model Parameter Extraction for Si Micro-Ring Modulators

Byung-Min Yu[1], Jeong-Min Lee[1], Yoojin Ban[1], Seong-Ho Cho[2], and Woo-Young Choi[1]
[1]Department of Electrical and Electronic Engineering, Yonsei University, Seodaemun-gu, Seoul 120-749, Korea
[2]High Performance Device Group, Samsung Advanced Institute of Technology, Yongin, Gyeonggi-do, 446-712, Korea

Paper Summary

Numerical values for three key model parameters that describe the transmission characteristics of Si micro-ring modulators are extracted from measurement results. Their dependence on bias voltages is determined and their accuracy is compared with simulation results.

Introduction

Optical interconnects can offer many advantages over conventional electrical interconnects such as much higher data rates, EMI insensitivity, and smaller sizes [1]. Si photonics is a promising technology for realizing optical interconnects since Si technology provides potential for low-cost manufacturability of photonic devices and easy integration with Si electronics [2]. In particular, Si micro-ring modulators (Si MRMs) have small footprints and low driving voltages and, consequently, are actively investigated as one of the key devices for realizing Si-photonic optical interconnects [3]. Very high-speed Si MRMs with relatively low driving voltages have been demonstrated [4, 5].

In order to establish Si MRM technology based on foundry services, it is essential that accurate and convenient-to-use Si MRM models are established and the numerical values for the parameters used in those models are extracted from fabricated devices. In this paper, we demonstrate the model parameter extraction process for the Si MRM.

Structure of Si MRMs

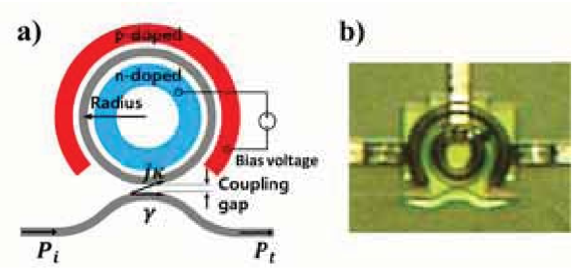

Fig. 1. a) Structure of Si MRM b) Chip photograph of Si MRM

Fig. 1 shows the structure of the Si MRM and the chip photograph of the Si MRM used in our investigation. The device is fabricated by IME Si-photonics foundry service through OpSIS [6] and implemented with 0.5-µm wide, 0.22-µm thick Si waveguides on 2-µm thick buried oxide layer. The Si MRM is composed of a ring resonator surrounded by the PN junction and a directional coupler. The ring radius is 8 µm and the coupling gap is 0.3 µm.

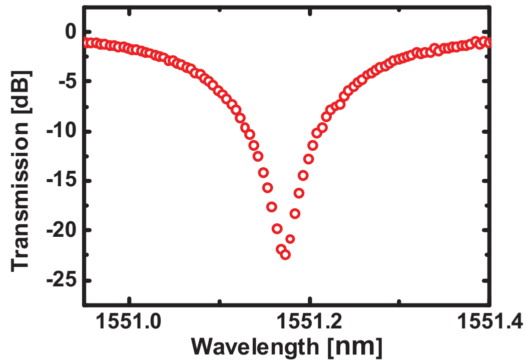

Fig. 2 Measured transmission characteristic of ring modulator (radius = 8 µm, coupling gap = 0.3 µm, bias voltage = 0 V)

Light injected into the device has the wavelength-dependent transmission characteristics. Fig. 2 shows the measured transmission characteristics for the Si MRM under investigation. For the measurement, light goes into and comes out of the device through fiber probes and grating couplers. The power of injected light is minimized so that Si MRM self-heating does not occur [7]. With reverse voltages applied across the p-n junction surrounding the ring resonator, the effective group index of the ring resonator waveguide can be modulated due to the change in the depletion width resulting in shifted resonance wavelength, which modulates the intensity of the injected light.

Parameter Extraction

The Si MRM transmission characteristic can be described with the following equation [8]:

$$T = \frac{P_t}{P_i} = \frac{\alpha^2 + \gamma^2 - 2\alpha\gamma\cos(2\pi n_{eff} L/\lambda)}{1 + (\alpha\gamma)^2 - 2\alpha\gamma\cos(2\pi n_{eff} L/\lambda)}. \qquad (1)$$

In the above equation, α represents the ratio of the optical power in the ring after one round-trip to the power before the round-trip. γ represents the through coefficient for the directional coupler. With κ, the direction coupler coupling coefficient, $\gamma^2 + \kappa^2 = 1$. n_{eff} is the effective group index of the ring waveguide. L is the circumference of the ring having the value of 50.26 µm for the device under investigation and λ is the wavelength of input light.

Our task is determining the numerical values of n_{eff}, α, and γ from measured transmission characteristics. n_{eff} can be easily determined from the resonance condition, $n_{eff} L = m\lambda_{res}$, where m is an integer. For our Si MRM, n_{eff}

Model Parameter Extraction for Si Micro-Ring Modulators

Byung-Min Yu[1], Jeong-Min Lee[1], Yoojin Ban[1], Seong-Ho Cho[2], and Woo-Young Choi[1]
[1]Department of Electrical and Electronic Engineering, Yonsei University, Seodaemun-gu, Seoul 120-749, Korea
[2]High Performance Device Group, Samsung Advanced Institute of Technology, Yongin, Gyeonggi-do, 446-712, Korea

Paper Summary

Numerical values for three key model parameters that describe the transmission characteristics of Si micro-ring modulators are extracted from measurement results. Their dependence on bias voltages is determined and their accuracy is compared with simulation results.

Introduction

Optical interconnects can offer many advantages over conventional electrical interconnects such as much higher data rates, EMI insensitivity, and smaller sizes [1]. Si photonics is a promising technology for realizing optical interconnects since Si technology provides potential for low-cost manufacturability of photonic devices and easy integration with Si electronics [2]. In particular, Si micro-ring modulators (Si MRMs) have small footprints and low driving voltages and, consequently, are actively investigated as one of the key devices for realizing Si-photonic optical interconnects [3]. Very high-speed Si MRMs with relatively low driving voltages have been demonstrated [4, 5].

In order to establish Si MRM technology based on foundry services, it is essential that accurate and convenient-to-use Si MRM models are established and the numerical values for the parameters used in those models are extracted from fabricated devices. In this paper, we demonstrate the model parameter extraction process for the Si MRM.

Structure of Si MRMs

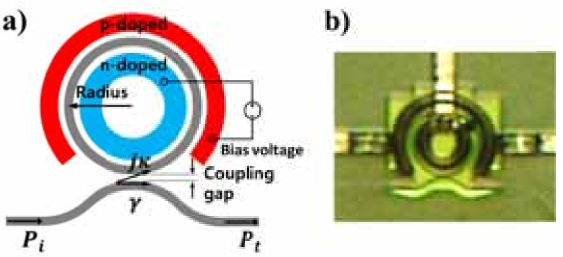

Fig. 1. a) Structure of Si MRM b) Chip photograph of Si MRM

Fig. 1 shows the structure of the Si MRM and the chip photograph of the Si MRM used in our investigation. The device is fabricated by IME Si-photonics foundry service through OpSIS [6] and implemented with 0.5-µm wide, 0.22-µm thick Si waveguides on 2-µm thick buried oxide layer. The Si MRM is composed of a ring resonator surrounded by the PN junction and a directional coupler. The ring radius is 8 µm and the coupling gap is 0.3 µm.

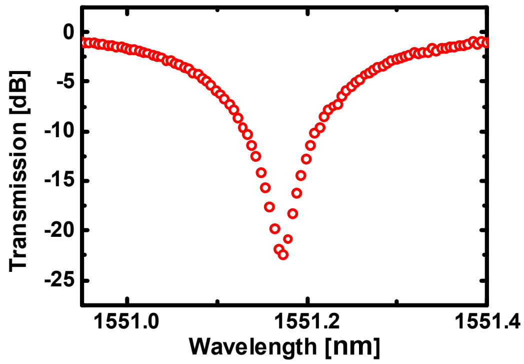

Fig. 2 Measured transmission characteristic of ring modulator (radius = 8 µm, coupling gap = 0.3 µm, bias voltage = 0 V)

Light injected into the device has the wavelength-dependent transmission characteristics. Fig. 2 shows the measured transmission characteristics for the Si MRM under investigation. For the measurement, light goes into and comes out of the device through fiber probes and grating couplers. The power of injected light is minimized so that Si MRM self-heating does not occur [7]. With reverse voltages applied across the p-n junction surrounding the ring resonator, the effective group index of the ring resonator waveguide can be modulated due to the change in the depletion width resulting in shifted resonance wavelength, which modulates the intensity of the injected light.

Parameter Extraction

The Si MRM transmission characteristic can be described with the following equation [8]:

$$T=\frac{P_t}{P_i}=\frac{\alpha^2+\gamma^2-2\alpha\gamma\cos(2\pi n_{eff}L/\lambda)}{1+(\alpha\gamma)^2-2\alpha\gamma\cos(2\pi n_{eff}L/\lambda)}. \qquad (1)$$

In the above equation, α represents the ratio of the optical power in the ring after one round-trip to the power before the round-trip. γ represents the through coefficient for the directional coupler. With κ, the direction coupler coupling coefficient, $\gamma^2 + \kappa^2 = 1$. n_{eff} is the effective group index of the ring waveguide. L is the circumference of the ring having the value of 50.26 µm for the device under investigation and λ is the wavelength of input light.

Our task is determining the numerical values of n_{eff}, α, and γ from measured transmission characteristics. n_{eff} can be easily determined from the resonance condition, $n_{eff}L = m\lambda_{res}$, where m is an integer. For our Si MRM, n_{eff}

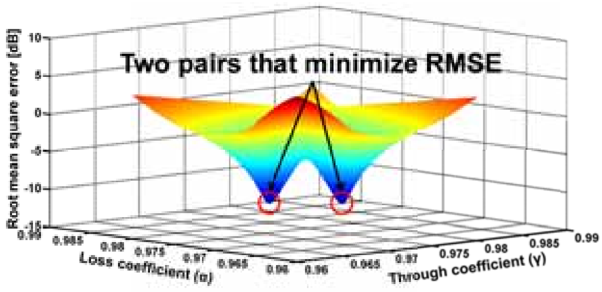

Fig. 3. RMSE dependence on α and γ

= 3.82659 when the reverse bias voltage is 0V. The numerical values for α and γ can be simultaneously extracted by fitting the measured data into Eq. 1 with the minimum mean squared error (MMSE) technique. Fig. 3 shows the resulting root mean squared error (RMSE) for different values of α and γ. As can be seen in the figure, there are two pairs of α and γ, (α = 0.9688, γ = 0.973) and (α = 0.973, γ = 0.9688) that produce the minimum RMSE. This is because interchanging α and γ in Eq. 1 produces the same result. The correct pair should be determined by performing additional measurement.

In MRMs, the transmitted power at the resonance wavelength becomes zero for critical coupling, which occurs when $\alpha = \gamma$. With the reverse bias applied, the depletion width increases and the light guided in the ring waveguide experiences less carriers, which increases α. However, γ does not change with the reverse bias since the directional coupler does not have any PN junction around it. Consequently, if $\alpha < \gamma$ for a given MRM, applying a reverse bias will produce less transmitted power at the resonance wavelength as it approaches critical coupling with increased α, but if $\alpha > \gamma$, the transmitted power at the resonance will be larger with a reverse bias [8]. The circles in Fig. 4 show measured transmission characteristics at three different biases. As can be seen, the transmitted power at the resonance decreases with the reverse bias indicating $\alpha < \gamma$ for our Si MRM. From this, we can choose the correct pair of (α = 0.9688, γ = 0.973) for the Si MRM with 0V bias. The

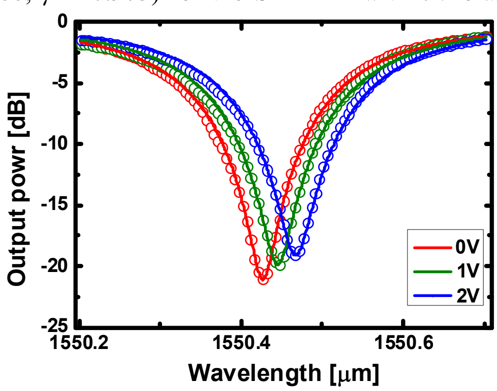

Fig. 4. Measured and fitted transmission characteristics

Bias voltage	α	γ	n_{eff}
0 V	**0.9688**	**0.973**	**3.82659**
−1 V	**0.9692**	**0.973**	**3.82664**
−2 V	**0.9695**	**0.973**	**3.82669**

Table 1. Extracted α and γ values

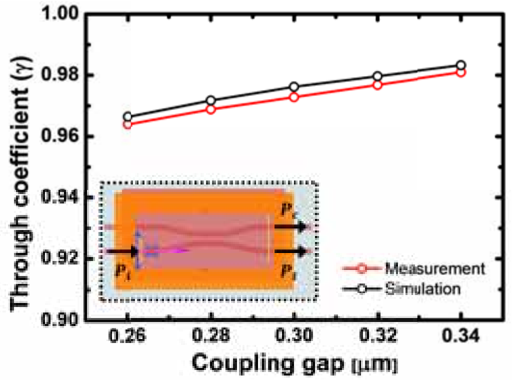

Fig. 5. Extracted γ from measurement and simulation

red line in Fig. 4 shows the calculated result from Eq. 1 with extracted parameter values. Similar process can be applied for the cases of −1 and −2 V biases and the results are shown in Fig. 4 and Table 1.

Comparison with Simulation

In order to check the accuracy of the extracted values, we experimentally extract γ values from five different Si MRMs having different couple gap values ranging from 0.26 μm to 0.34 μm and compare them with γ values determined from numerical simulation. For the simulation, Lumerical MODE Solution is used for the directional waveguides having the identical structure as in measured Si MRMs. Fig. 5 shows extracted and simulated γ values for different gap values. They agree well within about 0.2%. The slight difference is believed due to the fact that the fabricated waveguides do not have vertical sidewalls [9], which cause more coupling than vertical-sidewall waveguides used in simulation, resulting in less γ values.

Conclusions

We demonstrated the values for the key model parameters can be extracted from measured Si MRM transmission characteristics. We also compared the extracted values with simulation results.

References

1. M. Lipson *et al.*, Journal of Lightwave Technology Vol 23 No.12 (2005) 4222-4238
2. R. Ding, *et al.*, OFC/NFOEC Technical Digest (2012) OM2E.6
3. A. Ayazi *et al.*, Optics Express Vol. 20 No. 12 (2012) 13115-13122
4. G. Li *et al.*, Optics Express Vol. 19 No. 21 (2011) 20435-20443
5. T. Baba *et al.*, Optics Express Vol. 21 No. 10 (2013) 11869-11876
6. M. Hochberg *et al.*, IEEE Solid-State Circuits Magazine (2013) 48-58
7. X. Zheng *et al.*, Optics Express Vol. 20 No. 10 (2012) 11478-11486
8. W. Bogaerts *et al.*, LASER&PHOTONICS REVIEWS Rev. 6 No. 1 (2012) 47–73
9. T. Baehr-Jones *et al.*, OpSIS Design rule manual Version 2.61 (2013)